Optimum Dynamic Characteristic Control Approach for Building Mass Damper Design

2017 NZSEE Conference

S.J. Wang, B.H. Lee & Y.W. Chang

National Center for Research on Earthquake Engineering, Taipei, Taiwan.

K.C. Chang & C.H. Yu

Department of Civil Engineering, National Taiwan University, Taipei, Taiwan.

J.S. Hwang

Department of Civil and Construction Engineering, National Taiwan University of Science and Technology, Taipei, Taiwan.

ABSTRACT: A new seismic design manner, namely building mass damper (BMD), which comes from a combination of mid-story isolation and tuned mass damper (TMD) design concepts, recently attracts immense attention. In this study, an optimum building mass damper (OBMD) design approach, namely optimum dynamic characteristic control approach, is proposed to seismically protect both the superstructure (or tuned mass) and the substructure (or primary structure) respectively above and below the control layer. A series of sensitivity analyses and experimental studies on different parameters, including mass, frequency, and damping ratios, of a building designed with a BMD system were conducted. The test results verify the practical feasibility of the BMD concept as well as the effectiveness of the proposed OBMD design.

1 INTRODUCTION

The mid-story isolation design is recently gaining popularity owing to its advantages in terms of construction efficiency, space use, and maintenance over the conventional base isolation design. Previous researches have investigated the seismic responses of mid-story isolated buildings (Wang et al. 2012; Wang et al. 2013). It was indicated that the mid-story isolation design is effective in reducing the seismic demand of the superstructure above the isolation system if the coupling of higher modes is precluded. However, due to the flexibility of the substructure and the contribution of higher modes, the seismic response of the substructure below the isolation system may be enlarged.

Tuned mass dampers (TMDs) have been recognized as an effective passive energy absorbing device to reduce the undesirable oscillation of the attached vibrating system (or primary system) subjected to harmonic excitation (Den Hartog 1956; Luft 1979). Various approaches for selecting the optimum design parameters of such a system have been developed. For instance, to minimize the steady-state response of the primary system, Den Hartog (1956) derived the close-form solutions for the optimum tuning frequency and damping ratio of a TMD system attached to an undamped system under harmonic excitation. After that, Warburton (1982) studied the optimum TMD design parameters for an undamped system subjected to harmonic external force and white-noise random excitation. However, all systems contain some damping in reality. Tsai and Lin (1993) studied the optimum TMD design parameters for a damped system by numerical iteration and curve-fitting procedures. Sadek's criterion (1997) for seismic application was to select, for a given mass ratio, the tuning frequency and damping ratio that would result in equally large modal damping in the first two modes of vibration.

The TMD design concept was first adopted to mitigate the wind-induced vibration or enhance the serviceability of high-rise buildings, and was subsequently adopted to enhance the seismic capability of building structures. Until now, the effectiveness of the TMD design in reducing structural responses subjected to seismic loading is still arguable (Sladek & Klingner 1983), especially when the tuned mass is much smaller than the primary structure. To overcome the concern of limited response reduction due to insufficient tuned mass in the conventional TMD design, a new design concept,

namely building mass damper (BMD), was proposed and numerically studied in some researches. In the BMD system, as implied in the name, a part of structural mass, instead of additional mass, is intended to be an energy absorber. Ziyzeifar and Noguchi (1998) utilized an isolation layer composed of elastic bearings and viscous dampers to isolate a part of the structure in a tall building for versatile design goals. One of the goals was to reduce the seismic response of the substructure below the isolation layer by means of significant and out-of-phase movement of the isolated superstructure as a vibration absorber. In addition, based on the numerical results of a 13-story building subjected to various seismic excitations, Villaverde (2002) indicated that the insertion of flexible laminated rubber bearings and viscous dampers between the roof and the rest of the building, namely roof isolation system, can effectively reduce the seismic response of the building. That is, the roof isolation system was designed to be a vibration absorber.

The BMD concept has been applied to a few new constructions and retrofitted buildings; for instance, the Swatch Group Japan Headquarter in Tokyo and the Theme Building at the Los Angeles International Airport. However, among these applications, the control target was still focused on the substructure (or primary structure) performance rather than on either the superstructure (or tuned mass) performance or both. If the superstructure in the BMD design is intended to be used for occupancy as the substructure, excessive dynamic responses are not acceptable definitely. Under this circumstance, the seismic performance of both the substructure and superstructure should be paid attention.

In this study, to combine the advantages of seismic isolation and TMD designs, an optimum design method for a BMD system is investigated. A building structure designed with a BMD system is rationally assumed to be represented by a simplified three-lumped-mass structure model. Referring to Sadek's research (1997), the objective function is refined as that the three modal damping ratios obtained from the simplified structure model in the direction of interest are equally important and taken as an approximately equal value. Accordingly, the optimum building mass damper (OBMD) design parameters can be rationally determined based on the proposed optimum dynamic characteristic control approach. First, the influences of varied mass ratios and inherent damping ratios on the OBMD design parameters are quantitatively discussed. Then, a series of shaking table tests were performed to verify the feasibility of the BMD concept as well as the effectiveness of the proposed OBMD design on seismic protection of the building models.

2 ANALYTICAL STUDY

2.1 Simplified three-lumped-mass structure model

In this study, the BMD system is intended to be installed upon a multi-story substructure (or primary structure). The system is essentially composed of a multi-story superstructure (or tuned mass) as well as spring and dashpot elements for connecting the superstructure to the substructure. The stiffness and damping designed for the BMD system, of course, are provided by the spring and dashpot elements, respectively. A simplified three-lumped-mass structure model, in which the three lumped mass are respectively assigned at the superstructure (SUP), control layer (CL), and substructure (SUB), is rationally assumed to represent a building structure designed with a BMD system, as shown in Figure 1. For doing so, an excessive (or unreasonable) damping demand for the OBMD design owing to a significant superstructure-to-substructure mass ratio and neglect of flexibility of the superstructure can be precluded, which will be further discussed in Section 2.3. The equation of motion for the simplified structure model in the horizontal direction can be written as

$$\begin{aligned}
&\mathbf{M}\ddot{\mathbf{u}}+\mathbf{C}\dot{\mathbf{u}}+\mathbf{K}\mathbf{u}=\mathbf{M}\mathbf{R}\ddot{u}_g \\
&\Rightarrow\begin{bmatrix} m_1 & 0 & 0 \\ 0 & m_2 & 0 \\ 0 & 0 & m_3 \end{bmatrix}\begin{Bmatrix} \ddot{u}_1 \\ \ddot{u}_2 \\ \ddot{u}_3 \end{Bmatrix}+\begin{bmatrix} c_1+c_2 & -c_2 & 0 \\ -c_2 & c_2+c_3 & -c_3 \\ 0 & -c_3 & c_3 \end{bmatrix}\begin{Bmatrix} \dot{u}_1 \\ \dot{u}_2 \\ \dot{u}_3 \end{Bmatrix} \\
&+\begin{bmatrix} k_1+k_2 & -k_2 & 0 \\ -k_2 & k_2+k_3 & -k_3 \\ 0 & -k_3 & k_3 \end{bmatrix}\begin{Bmatrix} u_1 \\ u_2 \\ u_3 \end{Bmatrix}=-\begin{bmatrix} m_1 & 0 & 0 \\ 0 & m_2 & 0 \\ 0 & 0 & m_3 \end{bmatrix}\begin{Bmatrix} 1 \\ 1 \\ 1 \end{Bmatrix}\ddot{u}_g
\end{aligned} \tag{1}$$

where **M** = the generalized seismic reactive mass matrix; m_1, m_2, and m_3 = the generalized seismic reactive masses for the fundamental mode of vibration computed for a unit modal participation factor of the substructure, control layer, and superstructure, respectively ; **K** and **C** = the horizontal generalized stiffness and damping coefficient matrices, respectively; k_1 (c_1), k_2 (c_2), and k_3 (c_3) = the horizontal stiffness (viscous damping coefficients) for the fundamental mode of vibration of the substructure, control layer, and superstructure, respectively; **u** = the horizontal displacement vector relative to ground; u_1, u_2, and u_3 = the horizontal displacements of the substructure, control layer, and superstructure relative to ground, respectively; $\ddot{u}_g$ = the horizontal ground acceleration; and **R** = the earthquake influence vector. The equation of motion given in Equation (1) can also be expressed in terms of the nominal frequency ω_1, frequency (or tuning) ratio $f_i = \omega_i / \omega_1$ (i = 2, 3), mass ratio $\mu_i = m_i / m_1$ (i = 2, 3), and component damping ratio $\xi_i = c_i \Big/ \sum_{j=i}^{3} m_j \omega_i$ (i = 1~3), in which i and j = 1, 2, and 3 denote the substructure, control layer, and superstructure, respectively; and the nominal frequencies ω_1, ω_2, and ω_3 are defined as $\sqrt{k_1 / m_1}$, $\sqrt{k_2 / (m_2 + m_3)}$, and $\sqrt{k_3 / m_3}$, respectively.

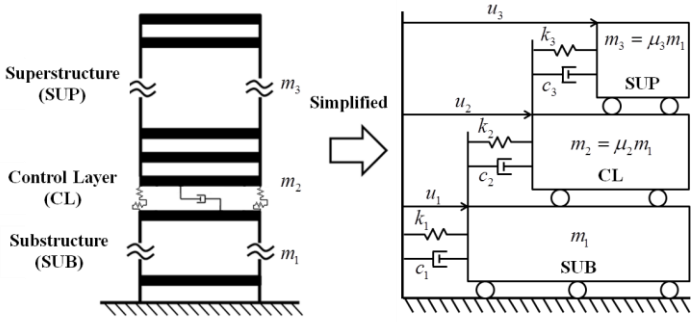

Figure 1. Simplified three-lumped-mass structure model for BMD design.

2.2 Optimum design method based on modal characteristic control concept

By means of the state space method under coupling approximation, the system matrix **A** for Equation (1) can be obtained. Accordingly, the complex eigenvalues can be calculated in a form of conjugate pairs. The proposed objective function to determine the OBMD design parameters in this study is modified from Sadek's research (1997). Three modal damping ratios which are dominant respectively for response mitigation of the substructure, control layer, and superstructure in the direction of interest are equally important and are taken as an approximately equal value, i.e. $\xi_1' \cong \xi_2' \cong \xi_3'$. Based on the proposed objective function with given ω_1, μ_2, μ_3, ξ_1, and ξ_3, the optimum design parameters for f_2, f_3, and ξ_2, i.e. f_2^{opt}, f_3^{opt}, and ξ_2^{opt}, respectively, can be determined.

2.3 Sensitivity analysis considering varied mass and damping ratios

Assume that the mass ratios μ_2 and μ_3 vary within a reasonable range respectively from 0.1 (i.e. basically representing a high-rise substructure) to 0.5 (i.e. basically representing a low-rise substructure) and 0.1 (i.e. basically representing a low-rise superstructure) to 2 (i.e. the story number of the superstructure is twice as many as that of the substructure). Besides, assume that both ξ_1 and ξ_3 are set to be 2% and 10% to correspondingly represent a bare structure and a structure with additional damping devices. Therefore, on the basis of the proposed objective function, the optimum damping ratio ξ_2^{opt} and the optimum frequency (or tuning) ratios f_2^{opt} and f_3^{opt} for the OBMD design varying with different μ_2, μ_3, ξ_1, and ξ_3 are calculated and shown in Figure 2. It can be seen that ξ_2^{opt}, f_2^{opt}, and f_3^{opt}, in general, are proportional to μ_2 and are inversely proportional to μ_3. This trend is less significant when μ_2 and μ_3 become larger gradually. It is implied that a decrease of μ_2 and an increase of μ_3 may reduce the OBMD design demands. In addition, ξ_2^{opt} will increase when ξ_1 is increased and will decrease when ξ_3 is increased. Increasing ξ_3 will lead to an increased demand of f_2^{opt} while will

reduce the demand of f_3^{opt}. On the other hand, the variation of the optimum frequency ratios with different ξ_1 is very sensitive to the mass ratios. When ξ_1 is increased, the demand of f_2^{opt} will generally decrease except for the nearly same trend at μ_2 equal to 0.1, and the demand of f_3^{opt} will decrease if μ_2 is small and will increase slightly with larger μ_2.

In Sadek's study (1997) and many past researches relevant to the TMD design, a simplified two-lumped-mass structure model was usually utilized to study the optimum TMD design parameters. Under this circumstance, only one mass ratio, i.e. a total of μ_2 and μ_3, was required to be defined. It was rarely concerned whether the damping demand is reasonable and practicable if the mass ratio becomes larger. As shown in Figure 3, the dotted line represents the trend of the optimum damping ratio varying with respect to the mass ratio obtained from Sadek's research (the inherent damping ratio is assumed to be 2%). It is found that the optimum damping ratio is proportional to the mass ratio, i.e. the larger the mass ratio, the higher the damping demand required. The solid lines represent the variation of the optimum damping ratio with different combinations of μ_2 and μ_3 when using the simplified three-lumped-mass structure model and the proposed optimum dynamic characteristic control approach (ξ_1=ξ_3=2%). Apparently, an opposite tendency that the optimum damping ratio, in general, is inversely proportional to the total of μ_2 and μ_3 but proportional to μ_2 is observed. More importantly, a more reasonable and applicable damping demand can be obtained especially when μ_2 becomes smaller.

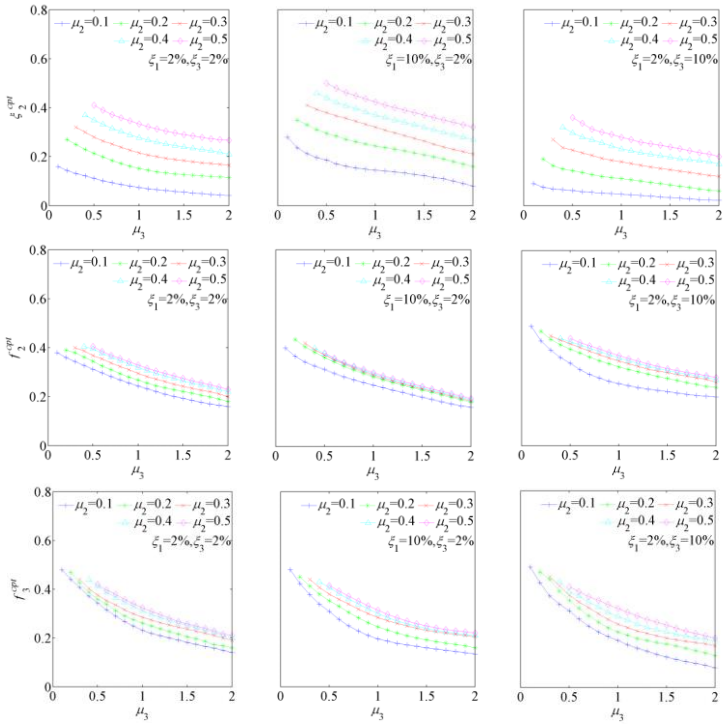

Figure 2. Optimum damping and frequency ratios with respect to μ_2, μ_3, ξ_1, and ξ_3.

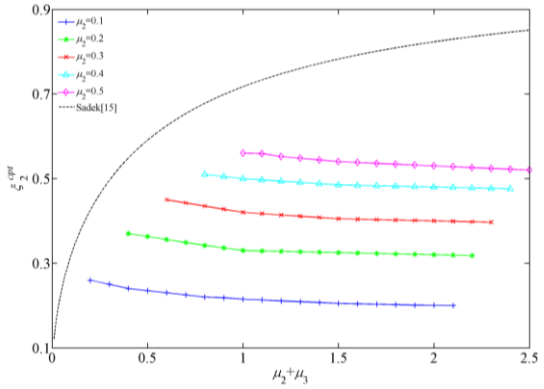

Figure 3. Optimum damping ratio obtained in Sadek's study (1997) and this study.

3 SEISMIC SIMULATION TESTS

3.1 Test structure models

The bare specimen was designed to be a 1/4 scaled 8-story steel structure model with single-bay widths of 1.5m and 1.1m respectively in the X and Y directions, as shown in Figure 4(a). Each floor was 1.1m high and each slab was 20mm thick. The columns and beams were wide flange with a sectional dimension of 100×100×6×8 (mm) and channel with a sectional dimension of 100×50×5×5 (mm), respectively. Additional live load of 0.5kN-sec^2/m simulated by mass blocks with a regular plane arrangement was assigned at each floor.

Apart from the bare specimen, the BMD specimens were designed with a control layer (CL) at the fourth floor, as shown in Figure 4(b). In other words, the substructure (or primary structure) and superstructure (or tuned mass) were three- and four-story structure models, respectively. In this study, for simplicity and practical feasibility, elastomeric bearings (RBs) with a diameter of 180mm and linear fluid viscous dampers (FVDs) were rationally adopted to play the roles of spring and dashpot elements at the control layer, respectively. A series of BMD specimens, i.e. BMD-1 to BMD-7 as given in Table 1, were designed to further discuss the influence of varying design parameters on their seismic performance. BMD-2, BMD-1, and BMD-3, the first-group specimens, were intended to only have different f_2 values in ascending order but the other design parameters remained the same. BMD-4, BMD-1, and BMD-5, the second-group specimens, were intended to only have different f_3 values in ascending order. BMD-6, BMD-1, and BMD-7, the third-group specimens, were intended to only have different ξ_2 values in ascending order.

The modal characteristics of the 8-story bare specimen, three-story substructure, and four-story superstructure were experimentally identified under white noise excitation. After obtaining the realistic characteristics, the optimum design parameters f_2^{opt}, f_3^{opt}, and ξ_2^{opt} for the OBMD specimen as shown in Figure 4(c) can be designed according to the proposed objective function with known ω_1, μ_2, μ_3, ξ_1, and ξ_3, as detailed in Table 1.

Table 1. Design parameters for all test and numerical structure models.

Specimen	ξ_2	f_2	f_3	Total stiffness at CL (4 sets of RBs)	Total rubber thickness of RBs	Total damping coefficient at CL (2 sets of FVDs)	Sectional dimension of added braces at substructure (SUB)
	(%)			(kN/m)	(mm)	(kN-sec/m)	(mm)
BMD-1	22	0.28	0.25	3810.28	27	51.12	L70×70×6 (SUB)
BMD-2	22	0.19	0.25	1740.52	19	34.56	L70×70×6 (SUB)
BMD-3	22	0.35	0.25	5880.00	19	63.76	L70×70×6 (SUB)
BMD-4	22	0.28	0.22	4905.20	20	58.00	L90×90×9 (SUB)
BMD-5	22	0.28	0.28	3247.72	30	47.20	L60×60×5 (SUB)
BMD-6	9	0.28	0.25	3810.28	27	20.92	L70×70×6 (SUB)
BMD-7	35	0.28	0.25	3810.28	27	81.34	L70×70×6 (SUB)
OBMD	25	0.30	0.28	1844.80	19	34.6	L60×60×5 (SUB)


(a) Bare specimen


(b) BMD specimen


(c) OBMD specimen

Figure 4. Experimental structure models.

3.2 **Input ground motions**

Four recorded ground motions, denoted as El Centro, Kobe, TCU047, and THU thereafter, with various peak ground acceleration (PGA) levels were selected for the earthquake inputs of the uniaxial shaking table tests (i.e. along the X direction of the specimens), as summarized in Table 2. Since the specimens were assumed as a 1/4 scaled structure model, a time scale of $1/\sqrt{4}$ was considered for the earthquake inputs to meet the similitude law. Note that the maximum test PGA level was determined on the premise of the specimens remaining essentially elastic.

Table 2. Earthquake test program.

Test name	Earthquake record	Original PGA	Test PGA / Original PGA	Bare specimen	BMD	OBMD
El Centro	El Centro/I-ELC270 Imperial Valley, USA 1940/05/19	0.35g	80%	V	V	V
			160%		V	V
			240%		V	V
Kobe	KJMA/KJM000 Kobe, Japan 1995/01/16	0.83g	40%	V	V	V
			60%		V	V
			80%		V	V
TCU047	Chi-Chi/TCU047 Chi-Chi, Taiwan 1999/09/21	0.40g	80%	V	V	V
			160%		V	V
			240%		V	V
THU	Tohoku/THU Tohoku, Japan 2011/03/11	0.33g	50%	V	V	V
			100%		V	V
			150%		V	V

3.3 **Influence of varying design parameters on seismic performance**

The maximum-acceleration ratio (AR_1) and maximum-inter-story-displacement ratio (IDR_1) of BMD-2, BMD-3, BMD-4, BMD-5, BMD-6, and BMD-7 to BMD-1, as calculated respectively in Equations (2) and (3), at different floors excluding the control layer (or 4F) are shown in Figure 5.

$$AR_1 = Max\ Acc_{BMD-i,\,j} \big/ Max\ Acc_{BMD-1,\,j} \tag{2}$$

$$IDR_1 = Max\ ID_{BMD-i,\,j} \big/ Max\ ID_{BMD-1,\,j} \tag{3}$$

where the subscript i = 2~7 represent BMD-2 to BMD-7; the subscript j represents the j^{th} floor (j = 1~8); $Max\ Acc_{BMD\text{-}i,\,j}$ and $Max\ ID_{BMD\text{-}i,\,j}$ represent the maximum acceleration and inter-story displacement responses at the j^{th} floor of BMD-i (i = 2~7), respectively; $Max\ Acc_{BMD\text{-}1,\,j}$ and $Max\ ID_{BMD\text{-}1,\,j}$ represent the maximum acceleration and inter-story displacement responses at the j^{th} floor of BMD-1, respectively.

As observed from these figures, in general, decreasing f_2 may cause enlarged acceleration responses at the substructure, while increasing f_2 may result in enlarged ones at both the substructure and superstructure, particularly for lower stories of the substructure and upper stories of the superstructure. Decreasing f_2 may cause enlarged inter-story-displacement responses at the superstructure, while increasing f_2 may result in enlarged ones at the substructure. Increasing f_3 may enlarge the acceleration responses of the substructure. Neither decreasing nor increasing f_3 causes significantly enlarged inter-story-displacement responses at the substructure and superstructure. It is of no surprise that the acceleration responses at both the substructure and superstructure of BMD-6 are larger than those of BMD-1 because of its smaller ξ_2. However, when ξ_2 becomes very large, e.g. ξ_2=35% in BMD-7, it may not be very helpful and even slightly harmful to the acceleration control performance compared to BMD-1 (ξ_2=22%). The influence of varying ξ_2 on the inter-story-displacement control at the substructure is more significant than that at the superstructure. Among BMD-1 to BMD-7 under all the earthquake excitation, the maximum inter-story displacement response at the control layer is 20.5mm, which is corresponding to a shear strain of 75.93% for RBs.

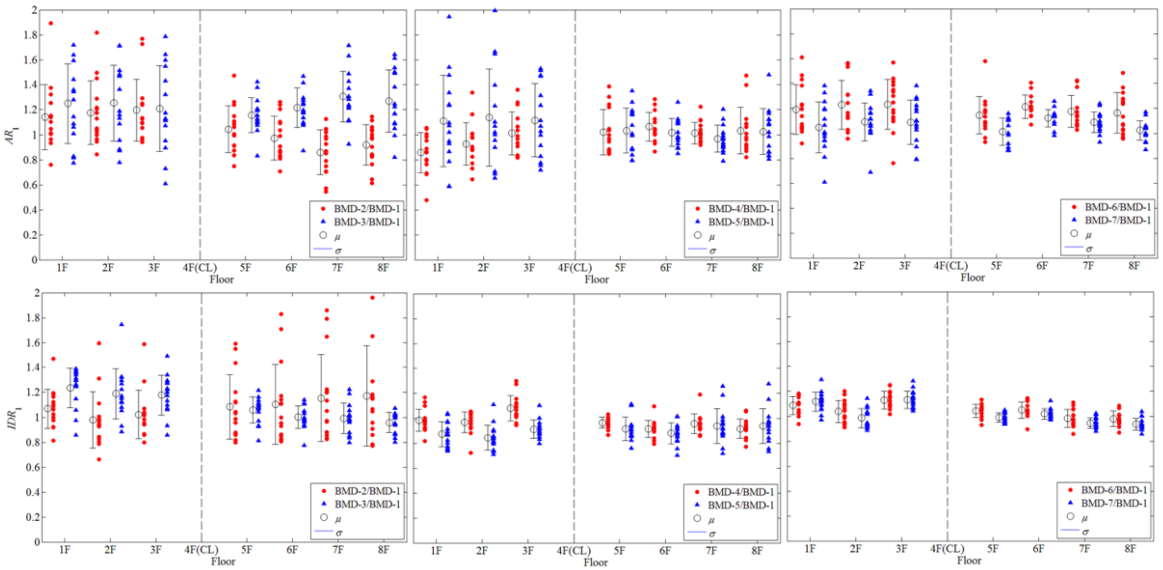

Figure 5. AR_1 and IDR_1 of BMD-2, BMD-3, BMD-4, BMD-5, BMD-6, and BMD-7 to BMD-1.

3.4 Comparison of seismic responses between bare, BMD, and OBMD specimens

The vertical distributions of maximum acceleration and inter-story displacement responses of the bare and OBMD specimens under 50% THU are presented in Figure 6, respectively. To statistically and overall demonstrate that the OBMD specimen designed based on the proposed objective function can have a superior seismic performance to the bare and BMD specimens, the average maximum-acceleration ratio (AR_2) and average maximum-inter-story-displacement ratio (IDR_2) of the bare and BMD specimens to the OBMD specimen, as calculated respectively in Equations (4) and (5), at the three-story substructure and four-story superstructure are shown in Figure 7.

$$AR_2 = Max\ Acc_{BMD-i,\,j}\,(\text{or } Max\ Acc_{Bare,\,j})\,/\,Max\ Acc_{OBMD,\,j} \tag{4}$$

$$IDR_2 = Max\ ID_{BMD-i,\,j}\,(\text{or } Max\ ID_{Bare,\,j})\,/\,Max\ ID_{OBMD,\,j} \tag{5}$$

where the subscript i = 1~7 represent BMD-1 to BMD-7; $Max\ Acc_{BMD\text{-}i,\,j}$, $Max\ Acc_{Bare,\,j}$, and $Max\ Acc_{OBMD,\,j}$ represent the maximum acceleration responses at the j^{th} floor of BMD-i (i = 1~7), the bare specimen, and the OBMD specimen, respectively; $Max\ ID_{BMD\text{-}i,\,j}$, $Max\ ID_{Bare,\,j}$, and $Max\ Acc_{OBMD,\,j}$ represent the maximum inter-story displacement responses at the j^{th} floor of BMD-i (i = 1~7), the bare specimen, and the OBMD specimen, respectively. Note that when the ratio is larger than unity and becomes higher, a better control performance of the OBMD specimen can be achieved.

As observed from these figures, the seismic performance of the OBMD specimen is much better than that of the bare specimen. In addition, the OBMD specimen has a superior potential in reducing the seismic responses to the BMD specimens, especially for the acceleration control performance at the superstructure as well as the inter-story displacement control performance at both the substructure and superstructure. It is experimentally demonstrated that the proposed optimum dynamic characteristic control approach for the OBMD design is effective and necessary. Under all the earthquake excitation as listed in Table 2, the maximum inter-story displacement response at the control layer of the OBMD specimen is 12.2mm, which is corresponding to a shear strain of 64.2% for RBs.

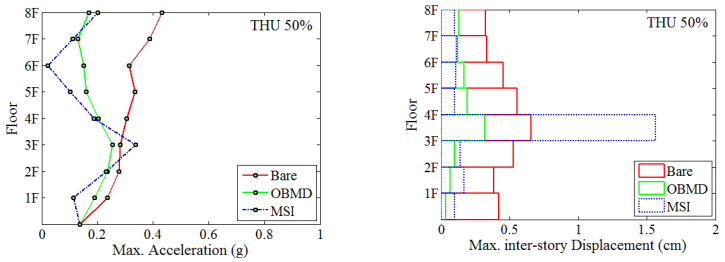

Figure 6. Vertical distributions of maximum responses of bare and OBMD specimens under 50% THU.

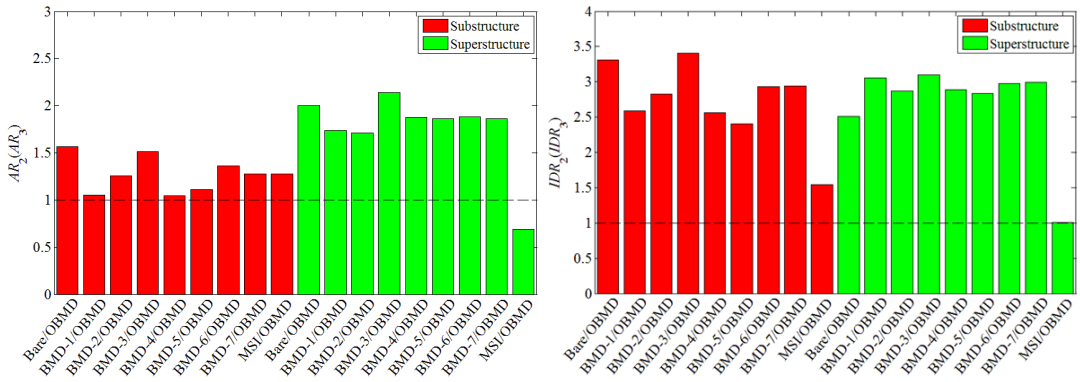

Figure 7. Average AR_2 and IDR_2 of bare and BMD specimens to OBMD specimen at SUB and SUP.

4 CONCLUSIONS

The objective function to determine the OBMD design parameters in this study is modified from Sadek's research (1997) and derived based on a simplified three-lumped-mass structure model. The sensitivity analysis results show a different trend for the optimum damping ratio varying with respect to the mass ratio from Sadek's study and many other past researches, i.e. the larger the mass ratio, the lower the damping demand required. Thus, by using the proposed optimum dynamic characteristic control approach to design a building with a BMD system, a reasonable and applicable damping demand can be obtained. The shaking table test results indicate that varying design parameters will cause entirely different seismic performances of a building with a BMD system. On the whole, moderately smaller f_2 and f_3 as well as larger ξ_2 can have a better control performance. Undeniably, however, the seismic performance of the BMD design, like the conventional TMD design, is strongly related to the frequency content of the seismic excitation. In addition, the proposed OBMD design has a superior potential in reducing the seismic responses of both the substructure and superstructure to the BMD design, which demonstrates the effectiveness and significance of the proposed optimum dynamic characteristic control approach. Undoubtedly, the seismic performance of the proposed OBMD design is much better than a counterpart without any structural control technology.

5 REFERENCES

Den Hartog, J.P. (4th edn). (1956). *Mechanical Vibrations*, NY: McGraw-Hill.

Luft, R.W. (1979). Optimum tuned mass dampers for buildings. *Journal of the Structural Division*, Vol 105: 2766-2772.

Sadek, F., Mohraz, B., Taylor, A.W. & Chung, R.M. (1997). A method of estimating the parameters of tuned mass dampers for seismic applications. *Earthquake Engineering and Structural Dynamics*, Vol 26(6): 617-635.

Sladek, J.R. & Klingner, R.E. (1983). Effect of tuned-mass dampers on seismic response. *Journal of Structural Engineering, ASCE*, Vol 109(8): 2004-2009.

Tsai, H.C. & Lin, G.C. (1993). Optimum tuned-mass dampers for minimizing steady-state response of support-excited and damped systems. *Earthquake Engineering and Structural Dynamics*, Vol 23(11): 957-973.

Villaverde, R. (2002). Aseismic roof isolation system: feasibility study with 13-story building. *Journal of Structural Engineering, ASCE*, Vol 128(2): 188-196.

Wang, S.J., Changm K.C., Hwang, J.S., Hsiao, J.Y., Lee, B.H. & Hung, Y.C. (2012). Dynamic behavior of a building structure tested with base and mid-story isolation systems. *Engineering Structures*, Vol 42: 420-433.

Wang, S.J., Hwang, J.S., Chang, K.C., Lin, M.H. & Lee, B.H. (2013). Analytical and experimental studies on mid-story isolated buildings with modal coupling effect. *Earthquake Engineering and Structural Dynamics*, Vol 42(2): 201-219.

Warburton, G.B. (1982). Optimal absorber parameters for various combinations of response and excitation parameters. *Earthquake Engineering and Structural Dynamics*, Vol 10(3): 381-401.

Ziyaeifar, M. & Noguchi, H. (1998). Partial mass isolation in tall buildings. *Earthquake Engineering and Structural Dynamics*, Vol 27(1): 49-65.